Self-consistent drift-diffusion model of nanoscale impurity profiles in semiconductor layers, quantum wires, and quantum dots

P. A. Sundqvist,[1,*] V. Narayan,[2] S. Stafström,[2] and M. Willander[1]
[1]*Physical Electronics and Photonics, Department of Physics, Fysikgränd 3, University of Göteborg and Chalmers University of Technology, S-412 96 Göteborg, Sweden*
[2]*Department of Physics, Linköping University, SE-581 83, Linköping, Sweden*
(Received 25 November 2002; published 30 April 2003)

We propose and model an experiment where impurity profiles in low dimensional structures can be controlled (during heat treatment) by an external parabolic potential defined by a variety of gate arrangements. At high temperatures the impurities are ionized and are able to move relatively quickly. After a realistic equilibrium time of typically one hour, the profiles are rapidly cooled such that the impurities are frozen in place. The model, which takes the electronic distribution as well as the mobile impurities into account results in a nonlinear Poisson equation. Similar models are widely used in semiconductor device theory where doping profiles are fixed. A parabolic potential in one, two, and three dimensions is applied to a semiconductor layer, a cylindrical quantum wire, and a spherical quantum dot, respectively. The impurity profiles are typically Gaussian shaped, where the distribution broadens with increasing temperature. The results demonstrate that the profile can be widely altered by changing the temperature, the average doping density, the size (radius), and the parabolic potential constant. The effect of parabolic confinement dimensionality on the diffusion is also studied. The temperature effect is studied up to a theoretical zero-temperature limit for which an analytic solution for the impurity profile is derived. The impurity profiles are sharper as the parabolic constant increases and the processing temperature is lowered. The processing time, however, increases exponentially as the temperature is lowered, and this must be considered in the practical situation.

DOI: 10.1103/PhysRevB.67.165330 PACS number(s): 66.30.Pa, 66.10.Cb, 66.30.Dn

I. INTRODUCTION

The physics of impurity diffusion in semiconductors has attracted a great deal of interest as most low dimensional structures (LDS's) have doped regions.[1] A number of variation calculations[2–5] have been performed to determine impurity binding energies in quantum wires. The confinement and the position of the impurities can dramatically alter the optical properties of the system. Furthermore, it has been been reported that the metallic doping of silicon can facilitate light emission from this material. Furthermore, a recent article has shown how layered doped silicon germanium nanowires can be grown.[6] Such structures will have interesting electron transport properties due to their (low) dimensions and their layered nature.

The impurities are usually introduced at high temperatures into LDS's, either by ion implantation,[7] diffusion,[8] or during molecular beam epitaxy (MBE).[9] The impurities ionize and experience a force in the presence of an electric field.[10] The experimental studies of impurities in linear potentials is well known.[11,8,12–14] Furthermore, the Coulomb repulsion between impurities will keep these ions apart and will impose a maximum doping level.[15] Recently, it was suggested that a nonlinear potential defined by a split gate arrangement can be used to trap impurities to regions of a semiconductor.[16,17] Here we consider alternative gate arrangements (previously used in quantum wire and dot systems to quantize the electronic states) to define impurity profiles in LDS's. It would be technologically very useful if impurity profiles can be controlled accurately and in a reproducible manner in LDS's. Furthermore, doping profiles are predicted using a drift diffusion model coupled to Poisson's equation.

Previously a split gate arrangement was considered which defined an approximately one-dimensional (1D) parabolic potential in a semiconductor layer.[18] Here other arrangements shall be investigated as well. A cylindrical quantum wire coated with a single gate will define a parabolic potential in two dimensions,[19] whereas a single square gate[20] can define a 2D parabolic potential in a semiconductor layer. We consider impurity diffusion in the presence of confining potentials in one dimension which can be achieved using the mentioned gate arrangements. In addition for completeness, impurity diffusion within a three-dimensional (3D) harmonic potential is also considered. A 2D and 3D generalization of the previous 1D Monte Carlo simulation would be time consuming. Therefore the problem is solved by coupling the drift-diffusion equation to the Poisson equation to obtain equilibrium doping profiles. The Monte Carlo method obtains time-dependent hopping probabilities using the microscopic Arrhenius equation[21–23] whereas the present approach is macroscopic in nature. The two approaches are essentially equivalent.[24] The drift diffusion approach previously used to model electrons and hole[25] has been applied to positrons[26] and hydrogen impurities[27] in electric fields.

In Sec. II we propose how the LDS can be fabricated experimentally. In Sec. III we give the general theory of the diffusion of the impurities and the nonlinear Poisson's equation. We also describe here the boundary conditions for the parabolic potential problem. In Sec. IV we present the numerical results for doping profiles prepared at high temperatures. Furthermore, a theoretical zero-temperature limit is

solved numerically for which an analytical approximate solution is derived. Finally, the conclusions are given in Sec. V.

II. PROPOSED EXPERIMENTS

The schematic diagram of the split gate arrangement is shown in Fig. 1(a). The gates define a potential which focuses the impurities to the center of the semiconductor layer during heat treatment (it is assumed that the impurities for the time scales considered have a relatively low probability of penetrating into the oxide). After the doping profile has reached equilibrium, the sample is quickly cooled so that the impurity profile is frozen. The split gate arrangements defines an approximately parabolic potential in the *y* direction. However, the curvature of the parabolic potential will also vary in the *z* direction.[18] The equilibrium and nonequilibrium doping profiles were previously predicted using Monte Carlo simulations. Here we shall predict the doping profile using a Drift-Diffusion analysis as a function of initial doping density, layer width, and temperature.

The schematic diagram of a gated quantum wire is shown in Fig. 1(b). This has been experimentally realized.[19] The gates define a 2D harmonic potential in the *x*-*y* plane. The impurities experience a force directed towards the center which results in a high concentration of impurities in the central area, as shown. The competing effect is the Coulomb repulsion between impurities that resist the buildup of charge into the central region. As before, after the doping profile has reached equilibrium the sample is rapidly cooled to freeze the doping profile. The gate can also be etched away if needed. One may also use a reverse bias on the gate of impurities with an opposite charge to localize charge around the edge. A number of variation calculations[2–5] have been performed to determine impurity binding energies in quantum wires. Our proposed experiment can create structures which can test these calculations.

The schematic diagram of a square gate above a semiconductor layer grown on top of a protective oxide layer is shown in Fig. 1(c). The square gate will define a potential that is harmonic in the *x*-*y* plane. When heated, the donors will migrate to a line in the *z* direction which passes through the center of the gate. After the impurity profile has reached equilibrium the sample is rapidly cooled. It was previously suggested that arrays of gates can be used to create modulation doped quantum dot arrays.

III. THEORY

This section is organized as follows. In subsection A we formally develop the nonlinear Poisson equation from the diffusion theory of dopants at high temperatures. The resulting equation is central to the semiclassical model for equilibrium semiconductors,[28] and is usually used for electrons and holes in doped semiconductors. In this model, we show that the impurities (which are fixed during device operation) play the same role as the holes for our problem, where the temperature is deliberately made very high so that the impurities are able to diffuse within a realistic time scale (typically around one hour). Crucially for controlling the impurity

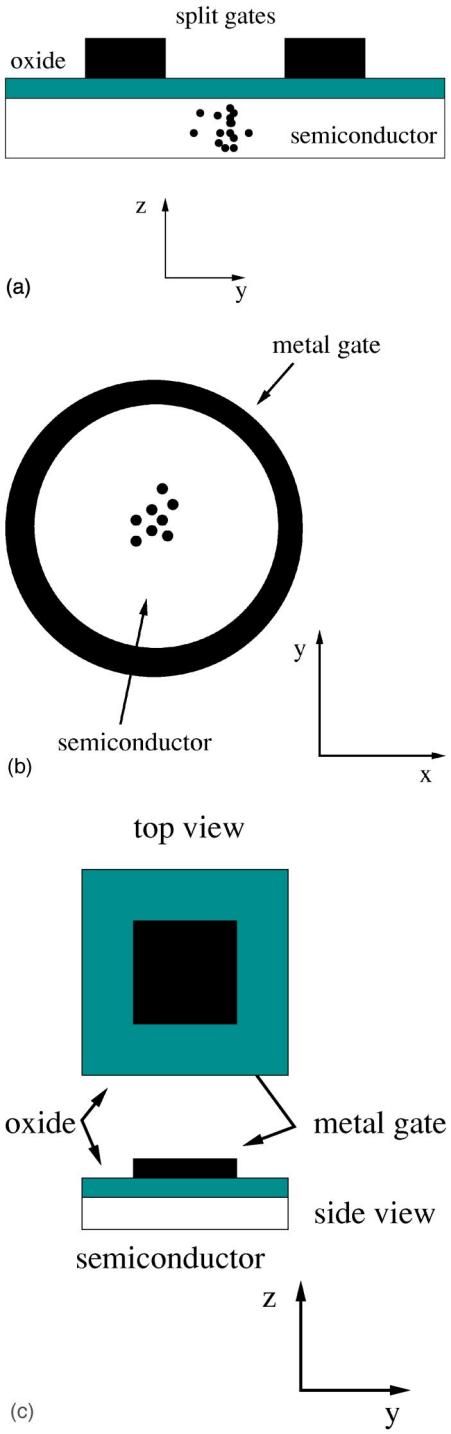

FIG. 1. (a) Proposed 1D split gate arrangement for creating a parabolic potential in a QW. The potential will, however, vary with the growth direction. (b) The cylindrical split gate on the top would create a 2D parabolic potential in a QWr. (c) An effective 3D external potential would be created in a thin QD region below the oxide layer.

profile we apply an external potential which is nonlinear (parabolic) to the donor-electron system. These two circumstances makes this problem quite different from a ''normal'' semiconductor electron and hole drift-diffusion theory. The system is in fact a mixed ionic-electronic conductor. This is

somewhat similar to oxygenated lithium compounds where the charge carriers consist of O^{2-} ions and holes.[29]

Subsection B deals with the boundary conditions that assure charge neutrality. In addition, we assume that the donor atoms are forbidden to diffuse into the protective oxide region (see Fig. 1). Finally, subsection C describes the numerical procedure to solve the nonlinear Poisson equation.

A. Diffusion and nonlinear Poisson theory

We consider a symmetrical structure in one, two, or three dimensions, and the boundary of the geometry for the general system is hence described by a *d*-dimensional radius R_d. The donors and the electrons are controlled by a *d*-dimensional symmetrical parabolic potential as well. For $d=1$ we have a quantum well (QW) with a maximum radius $R_1=L/2$ (where L is the width of the QW). It is surrounded by an oxide, which we approximate with a hard wall for simplicity. For $d=2$ we have a quantum wire (QWr), with cylindrical symmetry. At the maximum radius R_2 there is a protective oxide as well. Finally, for $d=3$ we have a spherical symmetric quantum dot (QD), with a radius R_3 (also surrounded by an oxide). Since the diffusion coefficient is strongly dependent on the temperature, the requested time to reach equilibrium could be manipulated by varying the temperature. At high temperatures, the positively charged donors and the electrons could be modeled using Maxwell-Boltzmann statistics. The equilibration time is at this high temperature reasonably short, typically less than 1 h. The next step in the process would be to keep the external potential on, meanwhile the LDS structure rapidly is cooled down to room temperature. When the LDS structure has been cooled down we could turn off the external potential, and the donors would be frozen. If we decrease the temperature down to room temperature, the diffusion constant will decrease by many orders of magnitude and the equilibration time would increase by many orders of magnitude as well. Evidently, this rapid cooling serves as a ''memory'' effect.

We consider here the simplest model where the diffusion coefficient D (for the donor atoms) is given by the Arrhenius equation

$$D=D_0 e^{-E_a/k_B T}, \tag{1}$$

where D_0 is constant of the order 1 cm^2/s and E_a is the activation energy of the order 3.5 eV for donors in Si. We also consider the Einstein relation to be valid, which relates the mobility μ of the carriers (where μ is inversely proportional to the mass) to the diffusion coefficient

$$D=\left(\frac{k_B T}{e}\right)\mu. \tag{2}$$

At high temperatures the donors are completely ionized. If they are placed in an external potential they will accelerate to minimize their energy, but will also diffuse according to a concentration gradient. All formalisms that have been developed for electrons (or holes) when deriving the drift-diffusion equation from the Boltzmann transport equations could hence be applied to the positively charged donors. The only difference between the donors and holes are then that the mobility is much smaller for the donors than for the holes, and in addition, the diffusion coefficient is very temperature sensitive [i.e., see Eq. (1)]. Further on this means that the relaxation time will depend on the temperature in the same way. The time-dependent drift-diffusion equations for the electrons could then be formulated for the electronic concentration n and for the donor density p as

$$\frac{\partial n}{\partial t}=\nabla\cdot\left(D_n\frac{en(\vec{r})}{k_B T}\vec{E}(\vec{r})+D_n\nabla n(\vec{r})\right), \tag{3}$$

$$\frac{\partial p}{\partial t}=\nabla\cdot\left(-D_p\frac{ep(\vec{r})}{k_B T}\vec{E}(\vec{r})+D_p\nabla p(\vec{r})\right), \tag{4}$$

where we have used the Einstein relation, Eq. (2), in the above equation. This drift-diffusion equation is one of the simplest ones, which excludes electron-hole generation rates and excess carriers. Further on we also notice that the electric field in Eqs. (3) and (4) could be determined from the electric potential Φ as $\vec{E}(\vec{r})=-\nabla\Phi(\vec{r})$. To determine the typical equilibration time we consider the following analysis in one dimension (in the y direction) for simplicity (a QW with width L). It is also useful to scale Eqs. (3) and (4). Let $y=L\cdot\xi$, $\varphi(y)=e\Phi(y)/k_B T$, and $d\tau=(D/L^2)dt$. With these scaling relations Eq. (3) would take the form

$$\frac{\partial n}{\partial \tau}=\frac{\partial}{\partial \xi}\left(-n\frac{\partial \varphi}{\partial \xi}+\frac{\partial n}{\partial \xi}\right). \tag{5}$$

The size of the system is now of the order of unity and the typical time τ it takes for the drift diffusion to equilibrate is hence roughly of the order of unity as well (the dominating time dependence in a diffusion equation is approximately given by $e^{-\tau}$). The real time it takes t_{fin} could, using the scaling relations and Arrhenius equation, be estimated as

$$t_{fin}=\frac{L^2}{D_0}e^{E_a/k_B T}. \tag{6}$$

For times much longer than t_{fin}, Eqs. (3) and (4) could safely be replaced with the stationary equations ($\partial n/\partial\tau=0$). For example, with As as a dopant in Si at $T=1220$ K and with a length $L=15$ nm the time would be 1 h. Here we use the values for As diffusion in Si, taken from Jaeger,[30] where $D_0=0.32$ cm^{-2} and $E_a=3.56$ eV. As a comparison, a temperature of $T=300$ K would correspond to 1.5×10^{41} years. For realistic times and temperatures Eq. (3) reduces to the stationary equation

$$-n\nabla\varphi+\nabla n=\text{const.} \tag{7}$$

With no stationary bias current [this would mean that the constant in Eq. (7) is set to zero], n and p (now scaled back again) are given by

$$n(\vec{r})=c_1 e^{e\Phi(\vec{r})/k_B T}, \tag{8}$$

$$p(\vec{r})=c_2 e^{-e\Phi(\vec{r})/k_B T}. \tag{9}$$

The constants c_1 and c_2 are determined to guarantee particle conservation. These equations verify that the drift-diffusion equations give the right Maxwell-Boltzmann distribution as the time goes to infinity. Note that the sign is opposite for the electrons and the donors in Eqs. (8) and (9). Also note that the Maxwell-Boltzmann distribution is the high-temperature limit of the Fermi-Dirac and Boze-Einstein distributions. More generally, the following classical condition must hold:

$$\frac{1}{N_{\mathrm{d}}}\left(\frac{mk_{\mathrm{B}}T}{2\pi\hbar^2}\right)^{3/2} \gg 1. \tag{10}$$

N_{d} is the doping density and m is the donor (or electron) mass. The interpretation of this inequality is that the thermal de Broglie wavelength must be much larger than the mean distance between the donors (or between the electrons). Ionized donors or acceptors could generally be either fermions or bozons,[31] but due to their heavy masses, their ''critical'' temperature T_{c} would be very low. For example, for As with $N_{\mathrm{d}}=10^{18}$ cm^{-3} and $m=74.9\,u$ the critical temperature would be $T_{\mathrm{c}}=0.4$ mK. An ionized As donor is a fermion in fact, since the remaining number of fermions is an odd number. The Fermionic critical temperature for the electrons (with the same doping concentration) would be $T_{\mathrm{c}}=55$ K, due to its small mass. For $T=1220$ K, the requested electronic density (the same as the donor density) would be $N_{\mathrm{d}}=1.0\times10^{20}$ cm^{-3} to violate the classical condition (for the electrons). In this case one should replace the Maxwell-Boltzmann distribution (only for the electrons) with the local Thomas-Fermi distribution (which require a calculation of the Fermi level) and in addition, for small structures (LDS's) one may instead use a Schrödinger-Poisson technique[32] to handle the electronic distribution in a satisfactory way. In this paper we work with reasonable doping densities and high temperatures. Therefore we use the Maxwell-Boltzmann distributions in all calculations.

So far we have neglected the Coulomb interaction. If for example the external potential is a parabolic potential (stopped at the boundary) the solution of Eq. (9) would be $\delta(\vec{r})$ as $T\to0$. This is of course not possible if we consider a many-electron system. To take the internal self-consistent interaction into account we have to replace $\Phi(\vec{r})\to\Phi_{\mathrm{ext}}(\vec{r})+\Phi_0(\vec{r})$, where the internal potential $\Phi_0(\vec{r})$ has to be determined by Poisson's equation,

$$\nabla^2\Phi_0(\vec{r})=-\frac{e}{\epsilon}[p(\vec{r})-n(\vec{r})]. \tag{11}$$

Using the charge densities given from Eqs. (8) and (9) into this equation would give

$$\nabla^2\Phi_0(\vec{r})=-\frac{e}{\epsilon}(c_2e^{-e\cdot[\Phi_{\mathrm{ext}}(\vec{r})+\Phi_0(\vec{r})]/k_{\mathrm{B}}T} - c_1e^{e\cdot[\Phi_{\mathrm{ext}}(\vec{r})+\Phi_0(\vec{r})]/k_{\mathrm{B}}T}). \tag{12}$$

This is the resulting nonlinear Poisson equation, which determines the internal potential. Once the solution of $\Phi_0(\vec{r})$ is known we can obtain n and p from Eqs. (8) and (9). So far everything has been general and we have not specified the geometry or the external potential for the system. Here we take the external potential to be parabolic. The parabolic constant could take either a fixed value or could be determined from an external potential V_0 at the boundary (i.e., at the d-dimensional radius R_{d}) as

$$\Phi_{\mathrm{ext}}=\left(\frac{V_0}{R_{\mathrm{d}}^2}\right)r^2=\frac{k}{2}r^2, \tag{13}$$

where r is the general radial coordinate. By using the Laplace operator in d dimensions, Eq. (12) becomes a one-dimensional problem,

$$\frac{1}{r^{d-1}}\frac{d}{dr}\left(r^{d-1}\frac{d\Phi_0(r)}{dr}\right)=-\frac{e}{\epsilon}(c_2e^{-e\cdot[\Phi_{\mathrm{ext}}(r)+\Phi_0(r)]/k_{\mathrm{B}}T} - c_1e^{e\cdot[\Phi_{\mathrm{ext}}(r)+\Phi_0(r)]/k_{\mathrm{B}}T}). \tag{14}$$

It is of great importance that the solution guarantees charge neutrality, otherwise the internal potential would grow to infinity far outside the low dimensional structure (LDS) (i.e., this happens for one and two dimensions but not for three dimensions, where net charges gives a $1/r$ contribution even in the oxide). This would be guaranteed if we use the following normalized distributions:

$$n=\frac{V_dN_{\mathrm{d}}e^{+\varphi}}{\int e^{+\varphi}dV_d}, \tag{15}$$

$$p=\frac{V_dN_{\mathrm{d}}e^{-\varphi}}{\int e^{-\varphi}dV_d}, \tag{16}$$

where N_{d} is the (mean) doping density and $\varphi=e[\Phi_{\mathrm{ext}}(r)+\Phi_0(r)]/k_{\mathrm{B}}T$ for a simpler notation. V_d is the d-dimensional volume $\{R_1,\pi R_2^2,4\pi R_3^3/3\}$ and dV_d is $\{dr,2\pi r dr,4\pi r^2dr\}$ for one, two, and three dimensions (remember that $R_1=L/2$, and that we only need to integrate in the half domain since the solution is symmetric).

B. Boundary conditions

To solve Eq. (14), we need to consider proper and meaningful boundary conditions on Φ_0. First, we note that the external potential is assumed to block both the electrons and the donors outside the LDS region, even though it does not appear in Eq. (13) explicitly, since we treat the oxide as a hard wall which then becomes our boundary and the external potential is assumed to vanish in this region as well. Strictly speaking we should use $\Phi(\vec{r})\to\Phi_{\mathrm{ext}}(\vec{r})+\Phi_0(\vec{r})+E_{\mathrm{v}}(\vec{r})$ for the holes/donors, where E_{v} is the valance band/semiconductor-oxide potential and $\Phi(\vec{r})\to\Phi_{\mathrm{ext}}(\vec{r})+\Phi_0(\vec{r})$

$+E_c(\vec{r})$ for the electrons, where E_c is the conduction-band/semiconductor-oxide potential.

Now we consider the boundary conditions for the parabolic potential. Since the solution is symmetric around $r=0$ we know that the derivate of Φ_0 has to be zero at this point. We may also choose the potential for the internal potential to be zero at the boundary. The boundary conditions could hence be summarized as

$$\Phi_0(R_d)=0, \tag{17}$$

$$\Phi_0'(0)=0. \tag{18}$$

Note also that the charge neutrality guarantees that the derivate of $\Phi_0'(R_d)=0$. Generally, for this kind of diffusion problem, the boundary condition should be homogeneous Neumann boundary conditions. This holds under the total charge neutrality condition since

$$\int\int\int_V \nabla\cdot(\epsilon\nabla\Phi_0)dv=\int\int_S \epsilon\nabla\Phi_0\cdot d\vec{S}= -e\int\int\int_V [p(\vec{r})-n(\vec{r})]dv=0. \tag{19}$$

Hence, $\nabla\Phi_0\cdot\hat{n}=0$ on the whole boundary surface. This boundary condition would then always guarantee that there is no net electric field generated outside the LDS region. Opposite, if the charge neutrality is violated, there would not exist a solution such that $\nabla\Phi_0\cdot\hat{n}=0$ on the whole surface and hence there will be electric field outside the LDS region (at least at some part of the surface).

C. Numerical method

The nonlinear Poisson equation [Eq. (14)] was solved numerical in the following way. The internal potential is solved self-consistently in an iterative way, and may be labeled $\Phi_{0,n}$ at the nth iteration. At the start $n=0$, and we set the internal potential $\Phi_{0,0}=0$ and then calculate the corresponding charge density ρ in the following way:

$$\varphi=\frac{e}{k_B T}\left(\frac{kr^2}{2}+\Phi_{0,n}\right), \tag{20}$$

$$\rho(r)=\frac{eN_d R_d^d}{d}\left(\frac{e^{-\varphi}}{\int_0^{R_d} e^{-\varphi}r^{d-1}dr}-\frac{e^{+\varphi}}{\int_0^{R_d} e^{+\varphi}r^{d-1}dr}\right). \tag{21}$$

The expression for the neutral charge density ρ is inserted into Eq. (14). If the resulting solution $\Phi_{0,n+1}$ is large compared to the external potential we take only a fraction of this solution and add it to the external potential. For example, for $d=1$ one finds that the analytic "start" solution $\Phi_{0,1}$ has its maximum value (at $r=0$) given by

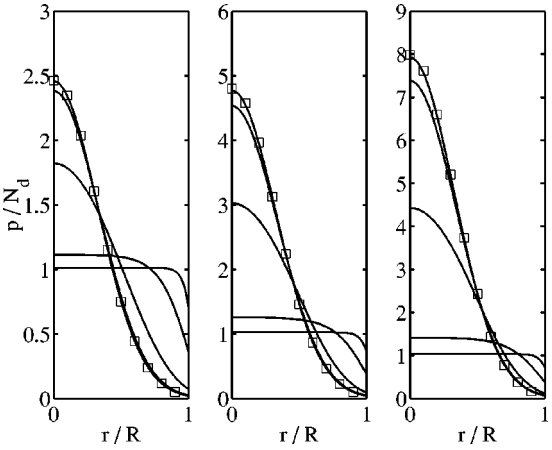

FIG. 2. The doping dependency of the equilibrium profiles for $T=1220$ K, $R=15$ nm, and $k=1/(15\times10^{-9})^2$ V/m^2. From left to right $d=1$, 2, and 3. From top to bottom, the mean doping densities are: $N_d=10^{16}$, 10^{17}, 10^{18}, 10^{19}, 10^{20} cm^{-3}. The local doping densities p are given as fractions of the mean doping density N_d. As a comparison, the squares indicates the "trivial" solution when the self-consistent internal potential Φ_0 is ignored.

$$\max(\Phi_{0,1})=\frac{N_d k_B T}{\epsilon k}\cdot\frac{2x}{\sqrt{\pi}} \times\frac{(1-e^{-x^2})[e^{x^2}erf(x)-erfi(x)]}{erf(x)erfi(x)}, \tag{22}$$

where $x=R/s$ and $s=\sqrt{2k_B T/ek}$. Thus if $\max(\Phi_{0,1}) \ll kR^2/2$ one can safely use a high increment fraction. Hence to perform a controlled convergence we take an increment ratio β to get the new $(n+1)$ potential

$$\Phi'_{0,n+1}=\beta\Phi_{0,n+1}+(1-\beta)\Phi_{0,n}, \tag{23}$$

where we use $\beta=0.1$ for $T\leqslant200$ K and $\beta=0.5$ for high temperatures. This new internal potential is then used in Eq. (20) and so on, until self-consistency is obtained, i.e., the solution does not change significantly. We use $\max(|\Phi_{0,n+1}(r)-\Phi_{0,n}(r)|)/\max[|\Phi_{0,n+1}(r)|]\leqslant10^{-6}$ as the stop criteria. It takes typically 20 and 40 iterations for convergence for high and low temperatures, respectively.

IV. NUMERICAL RESULTS

A. Profiles prepared at high temperature

We have solved Eq. (14) numerically for $d=1$, 2, and 3 and the impurity profile has been studied as a function of the doping density, temperature, radius, and parabolic constant. It should be noted that the parabolic constant (when appropriate) is set to be the same in all Cartesian directions (i.e., we assume that k does to not varies within the LDS region).

Figure 2 shows the equilibrium impurity profile as a function of doping density at $T=1200$ K for a QW, a QWr, and a QD ($d=1$, 2, and 3, respectively). The confining radius in the appropriate direction(s) is $R=15$ nm which corresponds to at least 50 monolayers since the lattice constant for most semiconductors is of the order 0.5 nm. Furthermore, the ex-

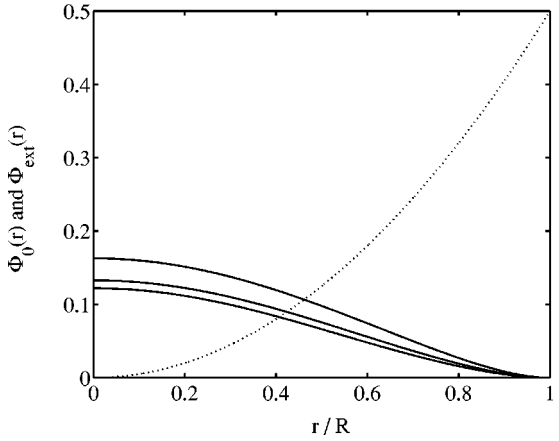

FIG. 3. The self-consistent internal potential Φ_0 (solid lines) is plotted as a function of r and is compared with the external (parabolic) potential Φ_{ext} (dotted line) for $d=1$, 2, and 3 from top to bottom. The parameters used were $T=1220$ K, $R=15$ nm, and $N_d=10^{18}$ cm^{-3} and $k=1/(15\times10^{-9})^2$ V/m^2.

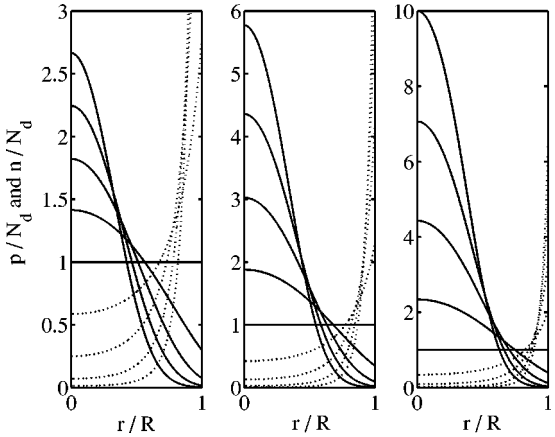

FIG. 4. The donor profile (solid lines) and the electronic profile (dotted lines) shown as a function of the parabolic potential constant k. Here, $T=1220$ K, $R=15$ nm, and $N_d=10^{18}$ cm^{-3}. For the donor profiles, the curvature becomes more sharply for stronger parabolic potentials, which is shown from bottom to top were k takes the values $k/k_0=0$, 0.5, 1.0, 1.5, and 2.0, where $k_0=1/(15\times10^{-9})^2$ V/m^2. For $k=0$ the self-consistent solution is flat both for the donor profile and for the electronic profile (the dotted line is not visible for this value of k). The electronic profile becomes more and more pushed up to the LDS walls as we increase the parabolic potential constant k. Notice that the electronic densities differ between $d=1$, 2, and 3. This is due to the different volume element, used in the particle conservation calculation.

ternal potential has a value of 0.5 V at the edge of the semiconductor. The squares in the figure show the ''start'' solution when the internal potential is equal to zero. The internal potential is proportional to the doping density [e.g., see Eq. (22)] and therefore a high doping density would generally generate a high internal potential so that it partly or almost could compensate for the external potential. In the opposite case, when the doping density is very low, the internal potential would be almost negligible in comparison with the external potential. A careful inspection reveals that the solution for low doping densities (10^{17} cm^{-3}) could be replaced with this ''trivial'' solution $p\propto\exp(-ekr^2/2k_BT)$. For medium doping densities (10^{18} cm^{-3}), the doping profile looks typically as a Gaussian distribution. For very high density (10^{20} cm^{-3}), the impurity profile is almost flat. If we work with a high doping density and we want a Gaussian-like distribution, we must significantly increase the parabolic potential constant k.

It is evident from Fig. 2 that increasing d results in a sharper profile. This may be understood through Fig. 3 where the internal potential $\Phi_0(r)$ is plotted and compared to the external parabolic potential. The results show that the internal potential typically looks like $\cos^2(\pi r/2R)$. Note also that the electric field at the boundary is equal to zero, which is a feature of a charge neutral system. We can therefore be assured that the numerical has been done correctly. For the shown ''typical'' case with $T=1220$ K, $N_d=10^{18}$ cm^{-3}, $R=15$ nm, and an external potential that equals 0.5 V at the semiconductor boundary, the internal potential decreases slightly with d. As an average, the ''response'' to the external potential is roughly 1/3 of the external parabolic potential. Note also that the thermal nonlinear response voltage $N_d k_B T/\epsilon k$ [defined in Eq. (22)] is 0.04 V for this case, while the maximum internal potentials is roughly 0.15 V. This indicates that the problem has to be solved self-consistently and that we can expect transient nonlinear phenomena.

The effect of the parabolic potential constant k is shown in Fig. 4 when all other parameters are fixed. In this figure we also analyze the electronic distribution. Here, $T=1220$ K, $N_d=10^{18}$ cm^{-3}, and $R=15$ nm. The parabolic potentials correspond to those that we apply 0–2 V at the edge. Evidently, no parabolic potential ($k=0$) results in a flat (bulk) distribution. For high parabolic potentials the impurity profile becomes sharply Gaussian formed. The electronic density becomes also more pushed up to the edges as k increases [i.e., this is more like an ''inverse'' Gaussian $1/\exp(-x^2)$]. Note here that the difference between the dimensions appears in the electronic distribution. Due to the weight factor r^{d-1} in the normalization integrals, a ''low'' electronic density close to the edge for $d=3$ is equal to a rather ''high'' electronic concentration for $d=1$.

In Fig. 5 we see the effect of changing the size of the low dimensional structure (i.e., this size is given by the d dimensional radius R_d). The almost flat impurity distribution corresponds to $R_d=2$ nm. It is particularly not realistic for a QD, where we can expect quantum effects to be very important. In addition the number of total impurities would be very few for such a small structure. We can of course expect quantum broadening to be important even in one and one dimensions. This figure shows, however, clearly the trend. A small structure would require a large parabolic potential to create a Gaussian-like distribution, to overcome the strong Coulomb repulsion.

B. Theoretical zero temperature limit

The influence of temperature is shown in Fig. 6 for an average doping level of 10^{18} cm^{-3} for the external potential that equals 0.5 V at the semiconductor boundary. An increase

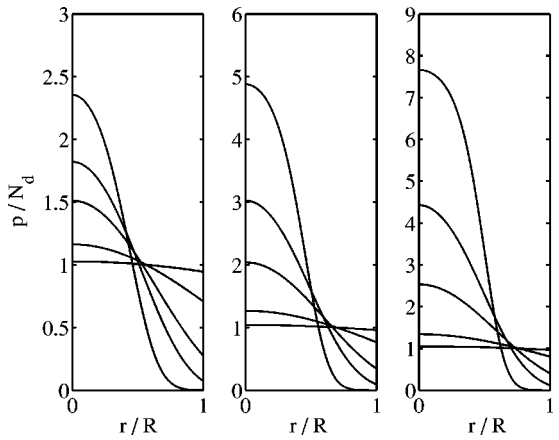

FIG. 5. The doping density profiles as a function of the ''radius'' in a QW, QWr, and QD are shown from left to right, when $T=1220$ K, $k=1/(15\times10^{-9})^2$ V/m^2, and $N_{\rm d}=10^{18}$ cm^{-3}. From bottom to top: $R=2$, 5, 10, 15, 30 nm. The doping profile becomes almost flat for a very small radius. To compensate for this broadening one must increase the parabolic potential sufficiently.

in temperature tends to broaden the impurity profile, since the mean kinetic energy wants to spread out the impurities. For $T=2000$ K, the profile has a paraboliclike profile, rather than a Gaussian profile. In the low-temperature limit (which is unrealistic for diffusion of impurities in semiconductors) the donors are localized within a certain radius determined by the doping density. Here we go down to $T=40$ K which is close to the condition for complete separation between donors and electrons. The corresponding electronic distribution is very closely located to the edge. Note that the maximum density (at $T=0$ K) is directly proportional to the dimensionality d. The shapes looks similar for $d=1$, 2, and 3, except that the ''critical'' radius is slightly larger for $d=3$ than for $d=1$.

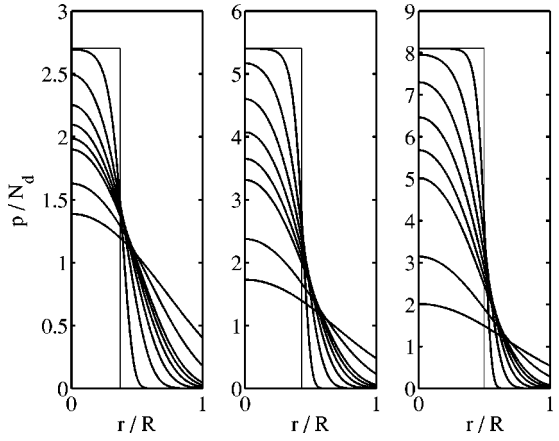

FIG. 6. The temperature dependence of the doping profiles are shown for $T=40$, 200, 400, 600, 800, 1000, and 2000 K, from top to bottom. The used parameters are $N_{\rm d}=10^{18}$ cm^{-3}, $R=15$ nm, and $k=1/(15\times10^{-9})^2$ V/m^2. From left to right $d=1$, 2, and 3. The thin lines indicates the theoretical distribution for the donors at $T=0$ K. The ''separation'' radii for $d=1$, 2, and 3 are given by $r/R=0.370$, 0.430, and 0.498 and with the corresponding maximum doping density $p/N_{\rm d}=2.70$, 5.40, and 8.11. The profiles becomes broader as the temperature increases.

An analytic solution of Eq. (14) would not generally be available for arbitrary dimensions. However, one could extract useful information of the system by taking the zero-temperature limit of the nonlinear Poisson equation. Indeed this is possible for an external parabolic potential as suggested by an inspection of the numerical solutions in the last figure, when the temperature was decreased. The result shows that the impurity density becomes flat inside a given radius, meanwhile the electronic density is pushed up exponentially to the boundary of the LDS, almost like a delta-dirac distribution. For this case, the positive donors and the negative electrons are completely separated from each other.

The explanation is that a homogeneous distribution contributes with a parabolic internal potential, which exactly cancels the external parabolic potential. Since the n and p distributions are totally separated one could solve the problem in each domain separately and match the internal potential at the separation radius R_0. For a homogeneous donor density p_0 in d dimensions, within the radius $0\leqslant r\leqslant R_0$ given as

$$p_0=N_{\rm d}\left(\frac{R_{\rm d}}{R_0}\right)^d, \tag{24}$$

we obtain the following solution of the Poisson equation:

$$\Phi_0(r)=a_0+a_1\Phi_{d,\,\rm hom}(r)-\frac{eN_{\rm d}}{2d\epsilon}\left(\frac{R_{\rm d}}{R_0}\right)^d r^2, \tag{25}$$

where $\Phi_{d,\,\rm hom}(r)$ is the homogeneous solution in d dimensions. Here we let the coefficient $a_1=0$, to obtain a self-consistent solution. Hence the sum of the external potential $(kr^2/2)$ and the internal potential would be zero if

$$\frac{R_0}{R_{\rm d}}=\left(\frac{eN_{\rm d}}{d\epsilon k}\right)^{1/d}. \tag{26}$$

Thus the corresponding doping level p_0 would be given by

$$\frac{p_0}{N_{\rm d}}=\frac{d\epsilon k}{eN_{\rm d}}. \tag{27}$$

Note that the condition $T\rightarrow0$ ensures that the electronic density within $0\leqslant r\leqslant R_0$ would be zero. The electronic distribution n in the domain $R_0\leqslant r\leqslant R_{\rm d}$ is in this temperature limit zero everywhere, except at $r=R_{\rm d}$, where it is infinite. Its corresponding internal potential is therefore linear in this region [i.e., it is given by $\Phi_{d,\,\rm hom}(r)$] except at $r=R_{\rm d}$, where its derivate changes discontinuously. This solution sets a limit of how high the (maximum) doping level can be and what the maximal curvature of the doping profile could be, when some parameters are kept fixed. It is also interesting to note that the dimensionality of the system could be characterized analytically with the number d. For example, Eq. (27) says that the maximal doping level is directly proportional to the dimensionality d. Of course, the electronic part of this solution is unrealistic due to quantum broadening in the electronic subband ground state.

V. CONCLUSIONS

In this paper we show that the diffusion theory of ionized impurities (interacting with electrons) at high temperatures could be explained with the same model as for holes and electrons using the semiclassical model for equilibrium semiconductors. In the ''normal'' semiconductor theory, the impurity profile is, however, kept fixed, which is normally the case for normal temperatures ($T \leqslant 1000$ K). As the temperature is kept high during the diffusion to create the special sharp (Gaussian like) impurity profile, a rapid cool down will ensure that this profile would be ''frozen'' at room temperature (and below) since the typical diffusion time depends exponentially upon the temperature. An external parabolic potential has been used to create an arbitrary sharp Gaussian impurity profile. The sharpness of the profile depends, however, also on the doping density and the temperature. We show that at high temperatures, small radii and large doping densities tends to broaden the impurity distribution. To overcome the Coulomb repulsion and the thermal broadening one has to increase the parabolic constant k sufficiently.

We find that the maximum donor density is directly proportional to the dimensionality for the system, so that a QD has a three times larger impurity concentration as a QW has at $r=0$. This effect is also explained with an analytic expression at $T=0$ K. In this paper we also analyze the type of boundary conditions that has to be used for this kind of diffusion problem.

The typical solutions uses values around $T=1200$ K, $R=15$ nm, and $N_d=10^{18}$ cm^{-2}, and we show that one can obtain typical Gaussian profiles, using split gate voltages of approximately 1 V. The model cannot be applied with confidence for small dimensions where quantum effect starts become important. Furthermore, a small number of impurities will be present and the mean-field approach in calculating the internal field would not be appropriate. We suggest that a previous Monte Carlo simulation of a limited number of impurities[33] in a delta doped layer can be modified to consider the diffusion of a small number of impurities within a 3D confining harmonic potential. The ideas presented in this paper can also be applied to control ion profiles in organic semiconductors. We hope that this paper stimulates future experimental work.

ACKNOWLEDGMENTS

The work was funded by SSF and the Carl Trygger Foundation.

*Email address: sunkan@fy.chalmers.se

[1] M. J. Kelly, *Low Dimensional Semiconductors* (Oxford University Press, Oxford, 1995).
[2] A. Latge, M. de Dios-Leyva, and L. E. Oliveira, Phys. Rev. B **49**, 10 450 (1994).
[3] A. Latge, N. Porras-Montenegro, and L. E. Oliveira, Phys. Rev. B **45**, 6742 (1992).
[4] P. Csavinszky and H. Oyoko, Phys. Rev. B **43**, 9262 (1991).
[5] D. S. Chuu and C. M. Hsiao, Phys. Rev. B **46**, 3898 (1992).
[6] L. J. Lauhon, M. S. Gudiksen, D. Wang, and C. M. Lieber, Nature (London) **420**, 57 (2002).
[7] S. M. Sze, *VLSI Technology* (McGraw-Hill, London, 1995).
[8] T. Sung, G. Popovici, M. A. Prelas, R. G. Wilson, and S. K. Loyalka, J. Mater. Res. **12**, 1169 (1997).
[9] E. F. Schubert, *Doping in III–V Semiconductors* (Cambridge University Press, Cambridge, England, 1993).
[10] G. E. Murch and A. S. Nowick, *Diffusion in Crystalline Solids* (Academic, Orlando, 1984).
[11] G. Popovici, T. Sung, S. Khasawinah, M. A. Prelas, and R. G. Wilson, J. Appl. Phys. **77**, 5625 (1995).
[12] J. C. Severiens and C. S. Fuller, Phys. Rev. **92**, 1322 (1953).
[13] C. S. Fuller and J. C. Severiens, Phys. Rev. **96**, 21 (1954).
[14] E. M. Pell, J. Appl. Phys. **77**, 291 (1954).
[15] E. F. Schubert, G. H. Gilmer, R. F. Kopf, and H. S. Luftman, Phys. Rev. B **46**, 15 078 (1992).
[16] V. Narayan and M. Willander, Phys. Rev. B **65**, 075308 (2002).
[17] V. Narayan and M. Willander, Phys. Rev. B **65**, 125330 (2002).
[18] Y. Sun, G. Kirczenow, A. S. Sachrajda, and Y. Feng, J. Appl. Phys. **77**, 6361 (1995).
[19] S. Bednarek, B. Szafran, and J. Adamowski, Phys. Rev. B **64**, 195303 (2001).
[20] A. Kumar, S. E. Laux, and F. Stern, Phys. Rev. B **42**, 5166 (1990).
[21] J. A. Combs and C. Kunz, Phys. Rev. B **36**, 289 (1987).
[22] W. G. Kleppman and R. Zeyher, Phys. Rev. B **22**, 6044 (1980).
[23] S. Fujii and Y. Uemura, Phys. Rev. B **40**, 1095 (1976).
[24] H. Gould and J. Tobochnik, *An Introduction to Computer Simulation Methods Part 2* (Addison-Wesley, London, 1988).
[25] M. Beck, D. Streb, M. Vitzethum, P. Kiesel, S. Malzer, C. Metzner, and G. H. Döhler, Phys. Rev. B **64**, 085307 (2001).
[26] M. P. Petkov, K. G. Lynn, and A. van Veen, Phys. Rev. B **66**, 045322 (2002).
[27] M. S. Jansen, A. Hallen, M. K. Linnarsson, and B. G. Svensson, Phys. Rev. B **61**, 7195 (2000).
[28] N. W. Ashcroft and N. D. Mermin, *Solid State Physics*, (Saunders College Publishing, Oxford, 1976).
[29] W. M. Saslow, Phys. Rev. B **59**, 15 160 (1999).
[30] R. C. Jaeger, *Introduction to Microelectronic Fabrication* (Modular Series on Solid State Devices (Addison-Wesley, Reading, MA, 1991).
[31] P. Ehrenfest and J. R. Oppenheimer, Phys. Rev. **37**, 333 (1931).
[32] J. H. Luscombe and A. M. Bouchard, Phys. Rev. B **46**, 10 262 (1992).
[33] N. S. Averkiev, M. A. Monakhov, A. Shik, P. M. Koenraad, and J. H. Wolter, Phys. Rev. B **61**, 3033 (2000).